Characterization of P3HT-CNT thin films for photovoltaic solar cell applications

Seithati Qotso[1*], Pontsho Mbule[2] and Bakang Mothudi[2]

[1]Department of Electrical Engineering, CSET, University of South Africa, Johannesburg, 1710, South Africa
[2]Department of Physics, CSET, University of South Africa, Johannesburg, 1710, South Africa

*E-mail: qotsoas@gmail.com / mbuleps1@unisa.ac.za

Abstract. This work report on the structure, morphology, optical and electrical properties of few-walled carbon nanotubes (FWCNT) as electron acceptor in the active layer of organic solar cell devices. FWCNT were dissolved in chlorobenzene and incorporated with pristine P3HT-conjugated polymer at different ratios (1:1-1:4) and systematically the effects on the structure, morphology, optical and photoluminescence were investigated. The XRD results exhibits the cubic structure, UV-Vis showed improvement in absorption which gives a better opportunity for enhanced efficiency in organic solar cells. PL results showed that all samples are quenching the P3HT intensity giving a large possibility of the charge separation in the photoactive layer and FESEM showed the disordered nanotubes.

1. Introduction

The global share of photovoltaic (PV) technologies in energy production still remains marginal today and is likely to remain this way for a long period of time especially in the poor developing countries [1]. The evidence of the limited global impact of PV is marked by the increasing market share of fossil fuels in the generation of electricity [2]. Carbon nanotubes (CNT) have emerged as one of the leading additives for improving the thermoelectric properties of organic materials due to their unique structure and excellent electronic transport properties [3]. CNT are the most commonly used and effective material among numerous fillers. They can provide conductive paths when embedded in polymer matrix since CNT possess excellent electrical conductivity and high charge mobilities [3]. These CNT can be divided into three (3) types: single walled carbon nanotubes (SWCNT), few walled carbon nanotubes (FWCNT) and multi walled carbon nanotubes (MWCNT) [4]. The high conductivity of CNT is due to the availability of free electrons owing to sp2 hybridized carbon atoms of the hexagonal graphite plane [5]. The electrical behavior of SWCNT can be determined by their chirality, either metallic or semiconductor [6], however, MWCNT is metallic if at least one sheet has a metallic chirality [7]. Comparing the CNT, FWCNT are known for their remarkable electronics properties [8], conductivity and field emission is stronger [9]. Jung et al. [10] incorporated FWCNT with different conducting polymers including poly(3 – hexylthiophene) (P3HT) for thermoelectric properties. They also reported the highest thermal conductivity when FWCNT incorporated with P3HT compared to other conducting

polymers. Khan et al. [11] used MWCNT mixed with P3HT as a photoactive layer for organic solar cells. In their findings, they reported the photoelectrical conversion efficiency (PCE) of 2.35%.

Recently, organic electronics based on conducting polymers have been intensively investigated due to their interesting band gap and they can also be easily used to fabricate thin films [11]. These conducting polymers have been applied in organic light emitting diodes (OLED), organic gas sensors (OGS) and organic solar cells (OSC) amongst others [12-16]. Poly(3 – hexylthiophene) P3HT is a conjugated electron donor polymer that is commonly used in solar cells, due to its good electro-optical properties, ease of process and synthesis [18–22] and it has been seen as the pillar in the development of future nanostructured polymer solar cells [23]. (P3HT) has been mostly applied in organic solar cells due to its narrow band gap (1.93-1.95 eV) that enable it to absorb a large energy spectrum [17]. In this study, P3HT-FWCNT at different ratios were investigated for the purpose of improving P3HT absorption and conductivity for applications in organic solar cells.

2. Experimental Procedure

Few walled carbon nanotube (FWCNT) and poly(3 – hexylthiophene) (P3HT) were purchased from Sigma Aldrich used in this study without further purification. FWCNT was dissolved in chlorobenzene using the ultrasonic bath for 30 minutes and P3HT was also dissolved in chlorobenzene and stirred on the magnetic stirrer for 24 hours. P3HT was incorporated in FWCNT at different ratios, the composites were stirred on the magnetic stirrer for 3 hours. The thin films were prepared by using a pipette to drop-cast the solution onto the ultrasonically cleaned borosilicate glass substrate and thereafter the film was then allowed to dry at room temperature. The thin films were then characterized using X-ray diffraction (XRD), ultraviolet to visible (UV-Vis/NIR) spectrophotometer and photoluminescence (PL) spectroscopy, field emission scanning electron microscopy (FE-SEM) and current-voltage (I-V) characterization.

3. Results and discussion

3.1. X-ray diffraction Analysis

Figure 1 shows the XRD results of the thin films prepared using the drop-cast method. The results show a clear cubic structure for all the samples. Furthermore, it clearly shows that by increasing the FWCNT-P3HT ratio, the intensity of the [302] peak decreases. The decrease in [302] intensity clearly shows that P3HT covers the surface of the FWCNT. The results shows that 1:1 ratio is more crystalline than other samples, and therefore the composite (1:1) are further studied by other techniques such as UV/Vis/NIR, SEM among others. The average crystallite size were found to be 19, 18, 16, 15 and 10 for FWCNT and P3HT-FWCNT at different ratios, respectively. The average crystallite sizes were calculated using the Scherrer equation [25]:

$$D = \frac{k\lambda}{\beta Cos\theta}$$

Where D is the crystallite size (nm), k is the Scherrer constant (0.9), λ is the wavelength of the x-ray source (0.15406 nm), β (radians) is the full width at half maximum and θ is the peak position in radians. It is clear that as the diffraction peaks broaden the crystallite size decreases.

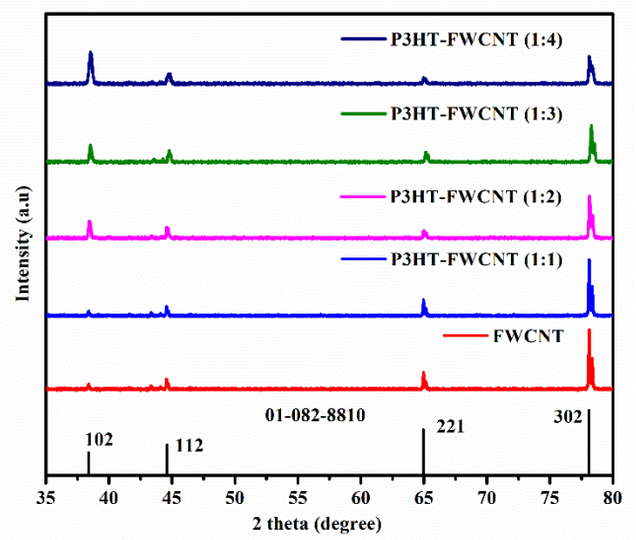

Figure 1: XRD patterns of FWCNT, P3HT, P3HT-FWCNT at different ratios.

3.2. UV-Vis Analysis

The absorption spectra of the prepared samples were investigated at room temperature using UV/Vis/NIR spectrophotometer in the wavelength region of 250 to 800 nm. Figure. 2 (a) shows the normalized absorption spectra P3HT and P3HT-FWCNT at different ratios. P3HT-FWCNT at different ratios show an improved absorption efficiency. The results clearly show that P3HT-FWCNT (1:1) has the highest absorption compared to other composites. This is expected to improve the electrical conductivity and may lead to the enhanced efficiency in photovoltaic solar cell. The spectra shows that the samples have peaks at different positions (530 and 636 nm), and these positions are attributed π-π* transitions of P3HT [26]. The optical bandgap was extrapolated from the linear portion of the Tau's plot [27]:

$$Ahv = A(hv\text{-}Eg)1/2, \quad (1)$$

where A is the constant, hv is the photon energy (h=Plank's constant and v is frequency of a photon) and a is the absorption coefficient. The estimated optical bandgap was obtained by extrapolating from the linear portion of the Tauc's plot as shown in figure 3 (b) with P3HT having 1.8 eV. The estimated bandgap for FWCNT was found to be 2.7 eV and 1.8-1.9 eV for P3HT-FWCNT at different ratios.

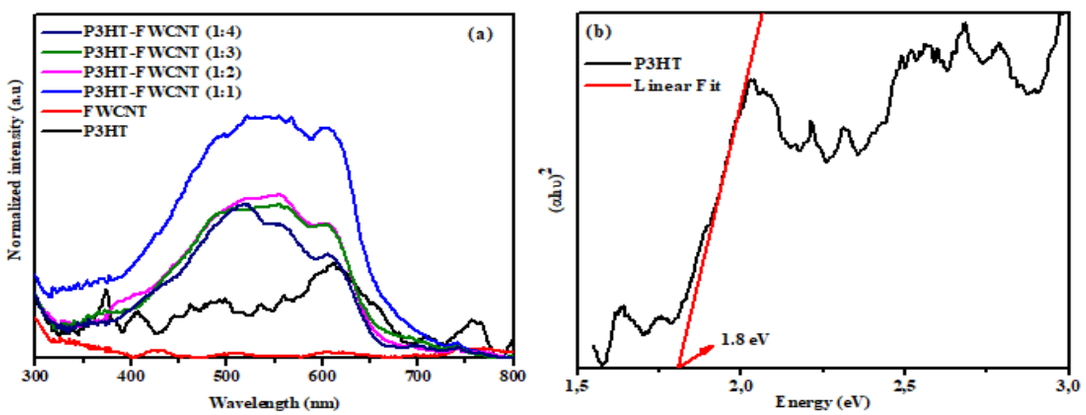

Figure 2: Normalized absorption spectra of (a) FWCNT, P3HT and P3HT-FWCNT at different ratios (b) P3HT Tauc's plot.

 ISBN: 978-0-620-97693-0

3.3. Photoluminescence Analysis

The PL measurements shown in Figure 3 (c) were carried out to observe the charge transfer between the donor-acceptor pair. The emission spectra were compared to that of P3HT. The PL results clearly shows PL quenching of the emission spectra, and this may be attributed to the presence of FWCNT. This confirms that charge transfer between P3HT and FWCNT was successful. This quenching is attributed to the position of P3HT LUMO and work function of FWCNT which are close to each other [28]. This phenomenon can be further explained by the strong π-π interaction between P3HT chains and FWCNT, through which the photoinduced electrons are efficiently separated and transferred and exitonic combination is avoided [29,30]. This makes it energetically favourable for electrons transfer from P3HT LUMO to FWCNT which suggest a strong electronic interaction between P3HT chains and FWCNT. These results correspond with UV/Vis/NIR results. The spectra shows that the samples have peaks at different positions (636 and 690 nm), and these positions are attributed to the pure electronic transition in the regioregular P3HT [31]. The results shows that P3HT-FWCNT (1:1) quenches the PL intensity even more showing a charge transfer between donor-acceptor materials and therefore reducing the electron-hole recombination. This P3HT-FWCNT (1:1) has a strong PL quenching effect which leads to a large possibility of charge separation in the photoactive layer.

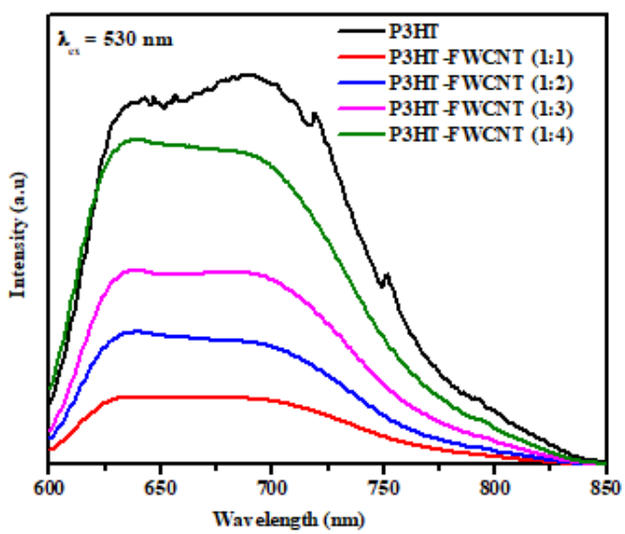

Figure 3: Emission spectra of pristine P3HT, and P3HT-FWCNT at different ratios.

3.4. FESEM Analysis

The FESEM images in figure 4 (a), (b) and (c) shows the morphology of the organic P3HT, nanotubes and disordered nanotubes, respectively. CNT performance in general is still not as impressive as expected due to some issues such as nanotube entanglement, non-alignment, and metallic impurities [32]. According to Danish et al. [32] these issues may lead to the decrement in hole mobility and increment in recombination pathways. However, in this study the aim is to search for the composite which has the strongest PL quenching effect which indicates the highest possibility of the charge separation in photoactive layer. Prior to choosing e an appropriate composition in the composite used for photoactive layer, we also investigated PL properties of pristine P3HT and composite film, and therefore 1:1 is expected to improve the electrical conductivity of P3HT.

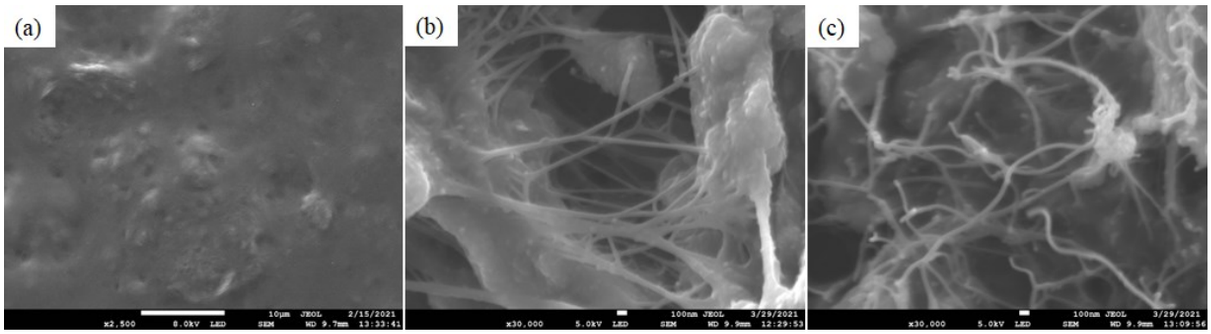

Figure 4: (a) P3HT (b) FWCNT (c) P3HT-FWCNT (1:1).

4. Conclusion

In summary, the interaction between FWCNT and P3HT have been studied. The XRD confirmed the cubic structure and that no other diffraction peaks other than those of FWCNT. UV-Vis showed improvement in absorption which gives a better opportunity for enhanced efficiency in organic solar cells. PL results showed that all samples are quenching the P3HT intensity giving a large possibility of the charge separation in the photoactive layer and FESEM showed the disordered nanotubes.

References

[1] Rwenyagila E.R 2017 *Int. J. Photoenergy.* 1–12.
[2] Grossiord N, Kroon M.J, R, Andriessen, Blom P.W.N 2012 *Org.Electron.* **13** 432–456.
[3] Qu S, Wang, Chen M. Y, Yao Q and Chen L 2018 *RSC.Adv*. **8** 33855–33863.
[4] McEuen P.L,Fuhrer M.S and Park H 2002 *IEEE Trans. Nanotechnol*, **1** 78–85.
[5] Inmuddin, Shakeel N, Ahamed M.I, Kanchi S and Kashmery H.A 2020 *Nature research*, **10** 5052.
[6] Dekker C, 1999 *Phys Today,* **52** 22 – 28.
[7] Stavarache L, Lepadatu A, Teodorescu V.S, Ciurea M.L, Lancu V, Dragoman M, Kostantinidis G, Buiculescu R, 2011 *Nanoscale Res. Lett.* **6** 88.
[8] Feng Y, Zhang H, Hou Y, McNicholas T.P, Yuan D, Yang S, Ding L, Feng W and Liu J 2008 *ASC Nan*o, **2** 1634–1638
[9] Ma M, Miao Z, Zhang D, Du X, Zhang Y, Zhang C, Lin J and Chen Q 2015 *Biosens. Bioelectron.* **64** 477–484.
[10] Jung J, Suh E.H, Jeong Y.J, Yang H.S, Lee T and Jang J, 2019 *ASC Appl. Mater. Interfaces,* S1–S14.
[11] Khanh T.S.T, Nam N.P.H and Dinh N. N 2020 *J. Mater. Sci: Chem. Eng*, **8** 1-10.
[12] Zhang M, Hofle S, Czolk J, Mertens A, Colsmann A, 2015 *Nanoscale,* **7** 20009 – 20014.
[13] Luo D, Chen Q.B, Liu B and Qui Y 2019 *Polymers,* **11** 384.
[14] Li G, Zhu R, Yang Y, 2012 *Nature Photonics*, **6** 153 – 161.
[15] Gao Y. Y, Wang Z, Yue G.T, Yu X, Liu X.S, Yang G, Tan F.R, Wei Z.X and Zhang W.F 2019 *Solar RRL,* **3** 1900012.
[16] Zhang Z.J, Miao J.H, Ding Z.C, Kan B, Lin B.J, Wan X.J, Ma W, Chen Y.S, Long X.J, Dou C.D, Zhang J.D, Liu J and Wang L.X 2019 *Nat.Commun.* **10** 3271.
[17] Ren S, Chang L.Y, Lim S.K, Zhao J, Smith M, Zhao N, Bulovic V, Bawendi M and Gradecak S 2011 *Nano Letters,* **11** 3998–4002.
[18] Haucha J. A, Schilinskya P, Choulisa S. A, Childersb R, Bielea M and Brabeca C. 2008 *J, Sol. Energy Mater. Sol. Cells* **92** 727 – 731
[19] Treat N.D, et al., 2011 *Adv. Energy Mater*. **1** 82 – 89.
[20] Liu C, Holman Z.C and Kortshagen U.R 2009 *Nano Lett.* 3 – 6.
[21] Greene L.E, Law M, Yuhas B.D and Yang P 2007 *J. Phys. Chem. C Lett.* 18.
[22] Chen D, Nakahara A, Wei D, Nordlund D and Russell T.P 2011 *Nano Lett*. 561 – 567.

[23] Dennler D, Scharber M.C and Brabec C.J 2009 *Adv mater* **21** 1323 – 1338.
[24] Ahmad M, Foroughi M and Monish M.R, 2012 *WJNSE*. **2** 154 – 160.
[25] Cullity B.D, Elements of X-ray Diffraction (2nd Ed), Addison Wesley, 1956, pp 284-285.
[26] Huiling T, Xian L, Yadong J, Guangzhong X and Xiaosong D 2015*Sensors.* **15** 2086 – 2103.
[27] Oh H, Krantz J, Litzov I, Stubhan T, Pinna L, Brabec C.J 2011 *Sol Energy Mater Sol Cells,* **95** 2194 – 2199.
[28] Lee J. M, Park J. S, Lee S. H, Kim H, Yoo S and Kim S. O 2011 *Adv. Mater.* **23** 629 – 633.
[29] Cheng F.Y, Imin P, Maunders C, Botton G and Adronov A 2008 *Macromolecules,* **41** 2304 – 2308.
[30] Jin H.D, Zheng F, Xu W.L, Yuan W.H, Zhu M.Q and Hao X.T 2014 *J.Phys. D: Appl. Phys* 505502.
[31] Al-Gaashani R, Radiman S, Daud A. R, Tabet N and Al-Douri Y 2013 *Ceram. Int*. **39** 2283 – 2292.
[32] Danish K, Zahid A, Danyal A, Manoj K.P, Idris K, 2021 *Ain Shams Eng. J,* **12** 897 – 900.